

Superconductivity in $\text{Hf}_5\text{Sb}_{3-x}\text{Ru}_x$: Are Ru and Sb a Critical Charge-Transfer Pair for Superconductivity?

Weiwei Xie,^{*,†} Huixia Luo,[†] Elizabeth M. Seibel,[†] Morten B. Nielsen,[‡] and Robert J. Cava^{*,†}

[†]Department of Chemistry, Princeton University, Princeton, New Jersey 08540, United States

[‡]Center for Materials Crystallography (CMC), Department of Chemistry and iNANO, Aarhus University, 8000 Aarhus C, Denmark

S Supporting Information

Superconductivity remains unpredictable for new compounds because, from the physics perspective, it results from instabilities in a compound's electronic system that are delicately balanced with other factors such as electron–lattice coupling or magnetism.¹ As such, there are few predictive rules that are thought to work more than they fail. One of these, perhaps the most long-standing, is that within intermetallic compounds of a known superconducting structure type, one can count electrons and expect to find the best superconductivity at 4.5 or 6.5 valence electrons per atom.^{2,3} This perspective can be considered a physicist's “rigid band” model where the structure type and electron count are held paramount; the actual atoms present are generally not a prime consideration.

But, from a chemical perspective, there have long been indications that there is much more to the presence or absence of superconductivity than just electron count and structure type. Simply put, there appear to be a handful of “critical pairs” of atoms in the periodic table, where it can be postulated that the balance between covalent and ionic bonding leads to just the right kind of charge transfer between the atoms so that the bond valence responds to perturbations from the other forces present to lead to a superconductor. In contrast to the quantitative k space or Fermi surface view often employed in the hunt for superconductivity, the concept of critical charge transfer pairs is clearly a qualitative, real space view of what can give rise to superconductivity; however, this can be an equally important and productive viewpoint, especially from the perspective of the synthetic chemistry.⁴ Many would agree, e.g., that clear examples of such critical charge-transfer pairs in the periodic table are Cu–O and Fe–As, with other possibilities hinted at as well.^{5–7}

We were therefore motivated to test the importance of chemical identity on superconductivity in intermetallic compounds. We began by looking at compounds of the type $(\text{Hf}/\text{Zr})_5(\text{Sb}_{3-x}\text{M}_x)$ where M is a transition metal and $x \sim 0.5$, which occur within the superconducting W_5Si_3 structure type (W_5Si_3 , $T_c = 2.7$ K). Importantly, the doping of M stabilizes this structure type and allows us to elucidate the effect of element identity only. Despite the stabilization of a superconducting structure type, no superconductivity had been found in such systems prior to this study. As shown in Figure 1(Upper), M and Sb form a bonded chain in these compounds, inside a column of Hf. The M atom is a small fraction of the atoms present, and so one might initially guess that it is a trivial contributor to the overall electronic structure of the compound. However, our electronic structure calculations, described below, indicate otherwise. Additionally, the calculations show the presence of a saddle point in the energy vs wavevector dispersion of one of the electronic states, which is a

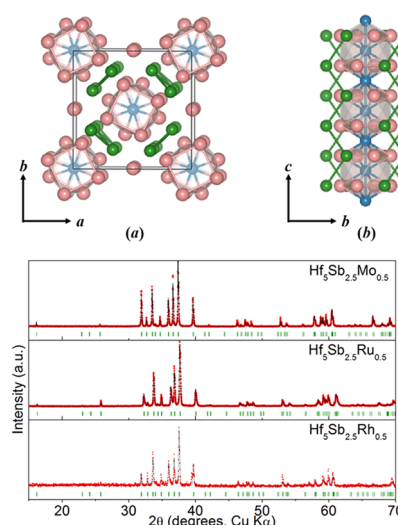


Figure 1. (Upper) The crystal structure of $\text{Hf}_5\text{Sb}_{2.54(4)}\text{Ru}_{0.46}$ in the W_5Si_3 -type structure. (a) a (001) view emphasizing the Hf square antiprisms around the 1:1 Ru/Sb chains. (Green: Sb; blue: Ru/Sb mixed chains; purple: Hf) and (b) a (100) “side view” of a column of Hf with the imbedded Ru–Sb chain. The Sb atoms surrounding the Hf column are also shown. (Bottom) Powder X-ray diffraction data showing the pure phases of W_5Si_3 -type $\text{Hf}_5\text{Sb}_{3-x}\text{M}_x$ ($M = \text{Mo}, \text{Ru}, \text{Rh}$). Red solid line shows the corresponding Rietveld fitting.

characteristic of band structures often taken to be a sign of impending electronic instability and a propensity toward superconductivity.⁸ Yet another factor in the recipe for superconductivity is often the suppression of magnetism. Ferromagnetism has been reported for $\text{Hf}_5\text{Sb}_{3-x}\text{M}_x$ when $M = \text{Fe}$, which implies that the 3d electrons may not be fully hybridized with the near neighbor Sb atoms and that this compound may sit near a critical atom-pair boundary. In such cases, the replacement of such a 3d for a 4d element can give rise to superconductivity because d electrons in 4d and 5d transition metals may hybridize with neighboring Sb atoms. This motivated us to search for stable compounds in the same structure type based on 4d rather than 3d elements. Naturally, our primary candidate for superconductivity was $M = \text{Ru}$.

Indeed, we find that the Ru variant $\text{Hf}_5\text{Sb}_{2.5}\text{Ru}_{0.5}$ is superconducting at 3.2 K; however, we do not find any

Received: May 4, 2015

Revised: June 11, 2015

Published: June 11, 2015

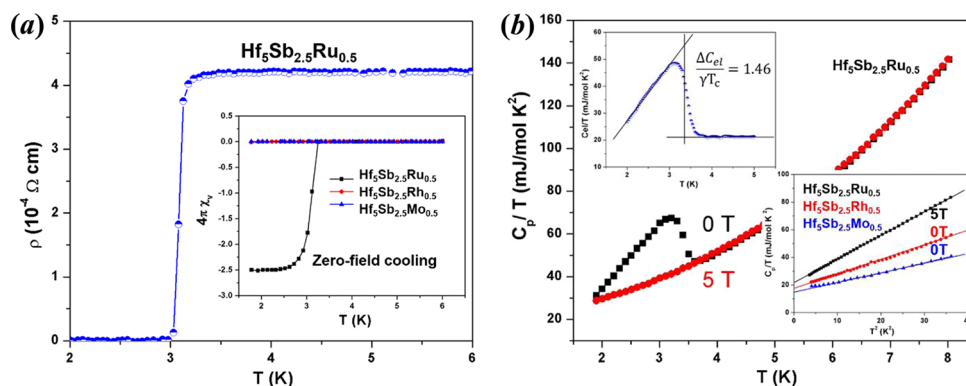


Figure 2. Physical properties measurements. (a) The electrical and magnetic properties of the $\text{Hf}_5\text{Sb}_{2.5}\text{Ru}_{0.5}$ superconductor. (Main panel) The temperature dependence of the electrical resistivity of $\text{Hf}_5\text{Sb}_{2.5}\text{Ru}_{0.5}$ in 0 applied magnetic field showing a close-up of the superconducting transition. (Inset) The temperature dependence of the magnetic susceptibility for $\text{Hf}_5\text{Sb}_{2.5}\text{M}_{0.5}$ ($\text{M} = \text{Mo}, \text{Ru}, \text{Rh}$) between 1.8 K and 6 K in an applied field of 10 Oe after zero-field cooling. (b) Specific heat characterization of the superconducting transition of $\text{Hf}_5\text{Sb}_{2.5}\text{Ru}_{0.5}$. (Main panel) Temperature dependence of the specific heat C_p of a $\text{Hf}_5\text{Sb}_{2.5}\text{Ru}_{0.5}$ sample measured with ($\mu_0 H = 5 \text{ T}$) and without a magnetic field, presented in the form of C_p/T vs T . (Inset, Lower) C_p/T vs T of $\text{Hf}_5\text{Sb}_{2.5}\text{M}_{0.5}$ ($\text{M} = \text{Mo}, \text{Ru}, \text{Rh}$) at applied fields of 0 ($\text{M} = \text{Mo}, \text{Rh}$) and 5 T (to suppress the superconductivity) fit to the form $C_p/T = \gamma + \beta T^2$; γ is the electronic contribution to the specific heat and βT^2 is the contribution of lattice vibrations. (Inset, Upper) The low temperature electronic heat capacity, as C_{el}/T vs T , in the temperature range 2.0–5.0 K; this is the “equal area construction” employed to determine the ratio of the change in entropy at the superconducting transition to the electronic specific heat (γ). C_{el} is determined by $C_p(\mu_0 H = 0) - \beta T^2$, where the latter part is the phonon part of the specific heat (see lower inset). The data show that $\text{Hf}_5\text{Sb}_{2.5}\text{Ru}_{0.5}$ is a high quality weak coupling BCS superconductor.

superconductivity present in the same structure type when Mo, Rh, Pd, or Pt is present in place of Ru, nor have others found it when the 3d elements V, Mn, Co, Fe, Ni, and Cu are present.⁹ Thus, of 11 transition elements tested, superconductivity is present for Ru only. Critically, we also do not find superconductivity when different atoms are cosubstituted as minor constituents to yield an isoelectronic band structure to $\text{Hf}_5\text{Sb}_{2.5}\text{Ru}_{0.5}$; ($\text{Hf}_{4.5}\text{Y}_{0.5}$) $\text{Sb}_{2.5}\text{Rh}_{0.5}$, for example, which is isostructural and isoelectronic with our superconductor, $\text{Hf}_5\text{Sb}_{2.5}\text{Ru}_{0.5}$, is not superconducting. These clear observations, along with the fact that the skutterudite $\text{LaRu}_4\text{Sb}_{12}$ is superconducting while isoelectronic and isostructural $\text{LaRh}_4\text{Sb}_8\text{Sn}_4$ is not, lead us to propose that Ru–Sb may be a third critical charge-transfer pair of elements for superconductivity in the periodic table along with Cu–O and Fe–As. Our work is described in detail in the following.

Polycrystalline $\text{Hf}_5\text{Sb}_{3-x}\text{Ru}_x$ samples were synthesized by arc melting the elements in a water-cooled copper hearth under an argon atmosphere using a tungsten electrode. The starting materials, hafnium (powder, 99.9%, Alfa Aesar), ruthenium (powder, 99.95%, Aldrich), and antimony (crystalline pieces, 99.999%, J&M), were weighed in the $\text{Hf}_5\text{Sb}_{3.0-x}\text{Ru}_x$ ($x = 0.0, 0.2, 0.4, 0.6, 0.8$, and 1.0) stoichiometric ratios (total mass 300 mg; 10% molar excess Sb added in order to balance Sb loss during the arc melting), pressed into pellets, and arc melted for 10 s. The products were turned and melted several times to ensure good homogeneity. Weight losses during the melting process were less than 2%. The products were stable in air and moisture. $\text{Hf}_5\text{Sb}_{3-x}\text{Ru}_x$ with $x = 0.0$ and 0.2 crystallizes in the Y_5Bi_3 -type structure; these materials are not superconducting and are not studied further here. With x in the range from 0.4 to 0.8 , the product adopts the W_5Si_3 -type structure, the subject of this work, whereas at higher doping levels ($x = 1.0$), an impurity phase, HfRu , appears in the final products. The as-melted $\text{Hf}_5\text{Sb}_{3-x}\text{Ru}_x$ samples were examined by powder X-ray diffraction for identification and phase purity on a Bruker D8 ECO powder diffractometer employing Cu $K\alpha$ radiation with aid of a full-profile Rietveld refinement using Fullprof.^{12,13} The phase in the powder pattern is a good fit to the $\text{Hf}_5\text{Sb}_{2.54(4)}\text{Ru}_{0.46}$ structural

model obtained from the single crystal study. The quantitative analysis of the powder diffraction pattern showed that the polycrystalline sample employed for the bulk property characterization consists of pure $\text{Hf}_5\text{Sb}_{3-x}\text{Ru}_x$ (see Supporting Information (SI) Figure 1(Bottom)). For the purposes of property comparison, $\text{Hf}_5\text{Sb}_{2.5}\text{M}_{0.5}$ ($\text{M} = \text{Mo}, \text{Rh}, \text{Pd}, \text{Re}, \text{Ir}, \text{Pt}$), $\text{Hf}_{4.5}\text{Y}_{0.5}\text{Sb}_{2.5}\text{Rh}_{0.5}$ and HfRu were prepared as pure phases by arc melting the elements in a stoichiometric ratio.

To specify the structure of the $\text{Hf}_5\text{Sb}_{3-x}\text{Ru}_x$ compound, single crystals extracted from arc melted samples were investigated on a Bruker Apex Phonon diffractometer with Mo radiation $K\alpha_1$ ($\lambda = 0.71073 \text{ \AA}$). The crystal structure was solved using direct methods and refined by full-matrix least-squares on F2 with the SHELXT package,^{14,15} and the chemical compositions of the $\text{Hf}_5\text{Sb}_{2.54(4)}\text{Ru}_{0.46}$ (hereafter referred to as $\text{Hf}_5\text{Sb}_{2.5}\text{Ru}_{0.5}$) crystals from the as-cast samples studied were confirmed by SEM-EDX chemical analysis performed on a Quanta 200 FEG ESEM operated at 20 kV. Temperature (T) dependent electrical resistivity (ρ) was measured from 1.9 and 300 K with the four-probe technique using silver paste electrodes on a Quantum Design Physical Property Measurement System (PPMS). Zero-field cooled (ZFC) magnetic susceptibility ($4\pi\chi_{\text{vol}}(T)$), measured in a field of 10 Oe using a Quantum Design superconducting quantum interference device (SQUID) magnetometer. Heat capacity was measured from 1.9 to 40 K on a PPMS by mounting pressed pellets of the samples on a sapphire platform with Apiezon N grease. The electronic structure was calculated using WIEN2k.¹⁶ The structures used to perform the calculations were based on full structural optimization results from VASP,¹⁷ starting with the experimentally determined structures. (Detailed calculations using LMTO methods for $\text{Hf}_5\text{Sb}_{2.5}\text{M}_{0.5}$ for $\text{M} = 3\text{d}$ transition metals have been described.⁹)

The refined crystal structure for $\text{Hf}_5\text{Sb}_{2.5}\text{Ru}_{0.5}$ is shown in Figure 1(Upper). This compound, and the others studied here, adopts the tetragonal W_5Si_3 -type structure (space group $I4/mcm$, Pearson Symbol $tP32$). Hf atoms are located at the $4b$ and $16k$ sites corresponding to the W sites in W_5Si_3 and Sb atoms fully occupy the $8h$ site. We have tested for the possibility of Sb/Hf mixed occupancy in the refinements and did not observe it to be

significant. The $4a$ sites are occupied by a nearly 1:1 mixture of Sb and Ru. The figure shows that the structure consists of Hf8 square antiprisms sharing their square faces to create columns along c , with linear chains of randomly mixed Ru/Sb atoms, in a nearly 1:1 ratio, imbedded inside them. The columns of square antiprisms are surrounded by Sb–Sb zigzag chains. The variability of Ru content allowed in the compound involves changes in the ratio of Ru to Sb in the linear chains. Detailed crystallographic data is presented in the SI. Inspection of the data in Tables S2 and S3 indicates that the equivalent isotropic displacement parameter of the $8h$ (Sb3) sites is lowest among the four positions in the asymmetric unit; our refinements show that this is not due to the presence of Hf/Sb mixing, and we note that relatively smaller displacement parameters are consistently observed at the $8h$ sites for $\text{Hf}_5\text{Sb}_{3-x}\text{M}_x$ ($\text{M} = \text{V}, \text{Mn}, \text{Fe}, \text{Ni}$).⁹

The temperature (T) dependent electrical resistivity for $\text{Hf}_5\text{Sb}_{2.5}\text{Ru}_{0.5}$ between 1.9 and 300 K is shown in Figure 2a. The resistivity undergoes a sudden drop to zero at 3.2 K, characteristic of superconductivity. In correspondence with $\rho(T)$, the magnetic susceptibility ($4\pi\chi_{\text{vol}}(T)$) starts to decrease at 3.2 K and shows large negative values, characteristic of a fully superconducting sample. The zero resistivity and the large diamagnetic susceptibility indicate that $\text{Hf}_5\text{Sb}_{2.54(4)}\text{Ru}_{0.46}$ becomes a bulk superconductor at 3.2 K. Critically, only the Ru doped compound shows the presence of superconductivity; $\text{Hf}_5\text{Sb}_{2.5}\text{M}_{0.5}$ ($\text{M} = \text{Mo}, \text{Rh}, \text{Pd}, \text{Re}, \text{Ir}, \text{Pt}$) shows no superconductivity. For example, $\text{Hf}_5\text{Sb}_{2.5}\text{Mo}_{0.5}$ and $\text{Hf}_5\text{Sb}_{2.5}\text{Rh}_{0.5}$ show only weak core-diamagnetism-dominated magnetic susceptibilities (Figure 2a, inset). To prove that the observed superconductivity is intrinsic to the $\text{Hf}_5\text{Sb}_{2.5}\text{Ru}_{0.5}$ compound, the superconducting transition was characterized further, through specific heat measurements. Specific heat measurements are a reliable indication of the presence of bulk superconductivity when combined with resistivity and susceptibility measurements due to the change in bulk thermodynamic properties at the superconducting transition. The specific heat for $\text{Hf}_5\text{Sb}_{2.5}\text{Ru}_{0.5}$ in the temperature range of 1.9 to 40 K is presented in Figure 2b. The main panel shows the temperature dependence of the zero-field and field-cooled specific heat C_p/T . The good quality of the sample and the bulk nature of the superconductivity are strongly supported by the presence of a large anomaly in the specific heat at $T_c = 3.2\text{--}3.3$ K, in excellent agreement with the T_c determined by $\rho(T)$ and $4\pi\chi_{\text{vol}}(T)$. The electronic contribution to the specific heat, γ , measured in a field of 5 T to suppress the superconductivity (lower inset to Figure 2b), is $21.92\text{ mJ}/(\text{mol}\cdot\text{K}^2)$. (The data are fitted using the formula $C_p = \gamma T + \beta T^3$, in which γ and β are the electronic and lattice contributions to the specific heat, respectively.) The value of the specific heat jump at T_c determined by the equal area method (upper inset Figure 2b), is consistent with that expected from a weak-coupling BCS superconductor: $\Delta C_{\text{el}}/\gamma T_c$ per mole $\text{Hf}_5\text{Sb}_{2.5}\text{Ru}_{0.5}$ in the pure sample = 1.46. This ratio is within error of the BCS superconductivity weak coupling value of 1.43 and is in the range observed for many superconductors.¹⁸ As an added check, we tested pure HfRu (The impurity that is present when the Ru content of a sample exceeds the solubility limit of the $\text{Hf}_5\text{Sb}_{3-x}\text{Ru}_x$ phase.) down to 1.78 K and found that it is not superconducting; that compound therefore could not give rise to the observed specific heat feature. Thus, the observed superconductivity originates from $\text{Hf}_5\text{Sb}_{2.5}\text{Ru}_{0.5}$. The figure (lower inset) also shows that the Ru–Sb compound has a significantly larger electronic contribution to the specific heat (γ) than the two comparison materials. The data indicates γ values of 21.9, 13.9,

and $15.9\text{ mJ}/(\text{mol}\cdot\text{K}^2)$ for the Ru–Sb, Mo–Sb, and Rh–Sb compounds, respectively. This parameter is a reflection of the density of electronic states at the Fermi energy and its renormalization due to electron–phonon coupling,^{19,20} and in the current case the large value for the Ru–Sb couple is an indication of the propensity for superconductivity.

To gain further insight into the uniqueness of $\text{Hf}_5\text{Sb}_{2.5}\text{Ru}_{0.5}$, we investigated the electronic density of states (DOS) and band structures of the hypothetical compounds “ $\text{Hf}_{10}\text{Sb}_5\text{M}$ ” (i.e., $\text{Hf}_5\text{Sb}_{2.5}\text{M}_{0.5}$; $\text{M} = \text{Fe}, \text{Ru}, \text{Mo}, \text{Rh}$) in space group $I422$, which allows the M–Sb chains to be modeled as M mixed with Sb in an alternating 1:1 ratio on what is the $4a$ site in the W_5Si_3 -type structure. This provides insight into the significance of the transition metal states near the Fermi energy (E_F) and the differences between 3d and 4d M systems. We first focus on the comparison between $\text{Hf}_{10}\text{Sb}_5\text{Fe}$ (3d) and $\text{Hf}_{10}\text{Sb}_5\text{Ru}$ (4d). The calculated DOS curves and band structures for these compounds are illustrated in Figure 3(a), which emphasizes contributions in

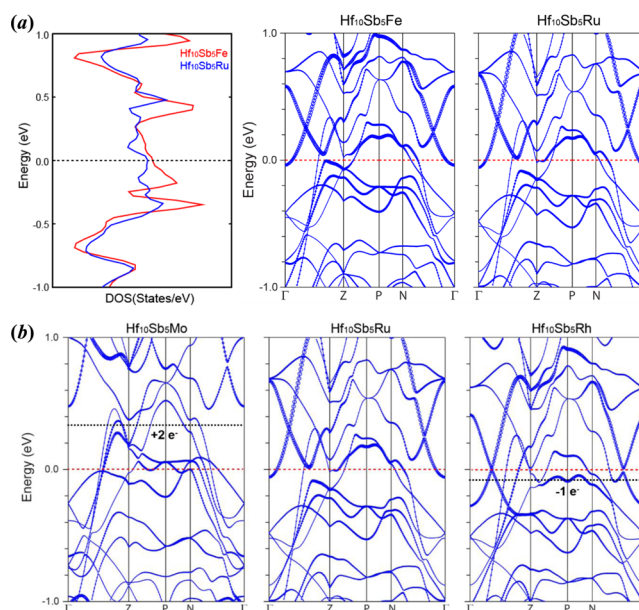


Figure 3. (a) Results of the electronic structure calculations for the hypothetical model compounds “ $\text{Hf}_{10}\text{Sb}_5\text{Ru}$ ” and “ $\text{Hf}_{10}\text{Sb}_5\text{Fe}$ ”. Total DOS curves and band structure curves are obtained from nonspin-polarized LDA calculations. (b) Results of the band structure calculations for hypothetical model compounds “ $\text{Hf}_{10}\text{Sb}_5\text{M}$ ” ($\text{M} = \text{Mo}, \text{Ru}, \text{Rh}$) obtained from nonspin-polarized LDA calculations. Ru calculation is a good representation of the superconducting phase. Red dashed lines show the Fermi levels for each compound, and black dashed lines show where the Fermi energy would fall when the appropriate number of electrons are added (Mo) or subtracted (Rh) to make these compounds have the same electron count as the Ru variant.

the range from -1 eV to $+1\text{ eV}$ of E_F . The significant DOS at E_F is consistent with the metallic properties of $\text{Hf}_{10}\text{Sb}_5\text{Fe}$ and $\text{Hf}_{10}\text{Sb}_5\text{Ru}$, and analysis of the orbitals contributing to the bands at E_F shows the dominance of the transition metal d states in this energy regime. Further, a saddle point is found near the N point in the Brillouin zone. The existence of such saddle points near E_F , called “van Hove singularities”, leads to the presence of peaks in the electronic DOS and is considered to be important in yielding superconductivity in a variety of superconductors, including oxo-cuprates, dichalcogenides, and even niobium.²¹ We hypothesize that this peak in the DOS remains present even

for a disordered or short-range ordered Ru–Sb chain structure. To test this hypothesis, we also calculated the electronic DOS for a chain arrangement of the type –Sb–Sb–Ru–Ru–, which may be present in small proportion in the material. The resulting DOS is shown in SI Figure S2. The peak in the DOS remains present. Thus, these initial electronic structure calculations confirm the appropriateness of this structure type for the test of our hypothesis—they indicate both the significant influence of the transition metal (*M*) electronic states at E_F , even though the *M* elements are a minor elemental constituent of the phase, and the presence of a peak in the electronic DOS, suggesting that superconductivity may be found. The calculations suggest that the 3d and 4d transition metal variants possess almost the same electronic picture.

Taking the argument one step further, we compare in Figure 3b the calculated band structures of $\text{Hf}_{10}\text{Sb}_5\text{M}$ (*M* = Mo, Ru, Rh) in this structure type to obtain information about why 4d transition metals other than Ru did not induce superconductivity. The band structure calculations show that E_F for the Ru-based compound locates close to the saddle point at N. Significantly, the saddle point at N is sensitive to the *M* element present—it is split into two bands for both the Mo and the Rh cases, that is to say, a “fingerprint” characteristic for superconductivity is not present as robustly in the Mo and Rh cases as it is for the Ru case. Our motivation for making the $\text{Hf}_{4.5}\text{Y}_{0.5}\text{Sb}_{2.5}\text{Rh}_{0.5}$ (i.e., $\text{Hf}_9\text{YSb}_5\text{Rh}$) compound is based on this observation. Removing one electron from $\text{Hf}_{10}\text{Sb}_5\text{Rh}$ puts E_F at the right position in the band structure to yield a compound that is structurally and electronically equivalent to $\text{Hf}_{10}\text{Sb}_5\text{Ru}$. We find, however, that $\text{Hf}_9\text{YSb}_5\text{Rh}$ is not superconducting.

In conclusion, we have shown that the $\text{Hf}_5\text{Sb}_{3-x}\text{M}_x$ family of compounds allows us to examine the hypothesis that chemical identity is important for superconductivity in intermetallic phases. We therefore propose that like Cu–O and Fe–As in other types of compounds, Ru and Sb represent a critical element pair for superconductivity in intermetallic compounds. This conclusion supplements the long-standing belief, based on a “rigid band” picture for intermetallics, that crystal structure and electron count (which, in a physics-based picture determine the Fermi surface) are the primary crystal-chemical requirements for the superconducting state in intermetallics, by adding another component for consideration. The work described here shows in general that when searching for new superconductors, even when given favorable electron counts and crystal structures, different but seemingly equivalent elemental constituents should be tested, simply because not all atoms are the same, even in superconductors.

■ ASSOCIATED CONTENT

■ Supporting Information

Single crystal data, atomic coordinates, and anisotropic thermal parameters of $\text{Hf}_5\text{Sb}_{2.54(4)}\text{Ru}_{0.46}$; powder XRD diffraction patterns of $\text{Hf}_5\text{Sb}_{3-x}\text{M}_x$ (*M* = Mo, Ru, Rh); DOS of $\text{Hf}_{10}\text{Sb}_5\text{Ru}$ with –Ru–Sb– and –Ru–Sb–Sb–Ru–Ru–Sb– linear chain; CIF of single crystal data of $\text{Hf}_5\text{Sb}_{2.54(4)}\text{Ru}_{0.46}$. The Supporting Information is available free of charge on the ACS Publications website at DOI: 10.1021/acs.chemmater.5b01655.

■ AUTHOR INFORMATION

Corresponding Authors

*(R.J.C.) E-mail: rcava@princeton.edu.

*(W.X.) E-mail: weiweix@princeton.edu.

Notes

The authors declare no competing financial interest.

■ ACKNOWLEDGMENTS

The chemical synthesis, single crystal diffraction, and electronic structure calculations were supported by the Department of Energy, Grant DE-FG02-98ER45706. The measurement and interpretation of the physical properties were supported by the Gordon and Betty Moore Foundation's EPiQS Initiative through Grant GBMF4412. M.B.N. gratefully acknowledges the Danish Ministry of Higher Education and Science for a travel scholarship for its support of his visit to Princeton.

■ REFERENCES

- (1) Poole, C. K.; Farach, H. A.; Creswick, R. J. *Handbook of Superconductivity*; Academic Press, 1999.
- (2) Cava, R. J. Oxide Superconductors. *J. Am. Ceram. Soc.* **2000**, *83*, 5.
- (3) Cherry, W. H.; Cody, G. D.; Cooper, J. L.; Cullen, G.; Gittleman, J. I.; Rayl, M.; Rosi, F. D. *Superconductivity in Metals and Alloys*; Rapid Corp of America: Princeton, NJ, U.S.A., 1963.
- (4) Norman, M. R.; Ding, H.; Randeria, M.; Campuzano, J. C.; Yokoya, T.; Takeuchi, T.; Takahashi, T.; Mochiku, T.; Kadowaki, K.; Guptasarma, P.; Hinks, D. G. Destruction of the Fermi Surface in Under-doped High- T_c Superconductors. *Nature* **1998**, *392*, 157.
- (5) Plakida, N. *High-Temperature Cuprate Superconductors: Experiment, Theory, and Applications*. Springer Science & Business Media: 2010.
- (6) Kamihara, Y.; Watanabe, T.; Hirano, M.; Hosono, H. Iron-Based Layered Superconductor $\text{La}[\text{O}_{1-x}\text{F}_x]\text{FeAs}$ ($x = 0.05\text{--}0.12$) with $T_c = 26$ K. *J. Am. Chem. Soc.* **2008**, *130*, 3296.
- (7) Rotter, M.; Tegel, M.; Johrendt, D. Superconductivity at ~ 38 K in the Iron Arsenide $\text{Ba}_{1-x}\text{K}_x\text{Fe}_2\text{As}_2$. *Phys. Rev. Lett.* **2008**, *101*, 107006.
- (8) Simon, A. Superconductivity and Chemistry. *Angew. Chem., Int. Ed. Engl.* **1997**, *36*, 1788.
- (9) Kleinke, H.; Ruckert, C.; Felser, C. Mixed Linear (*M*, Sb) Chains in the New Antimonides $\text{Hf}_{10}\text{M}_8\text{Sb}_{6-8}$ (*M* = V, Cr, Mn, Fe, Co, Ni, Cu): Crystal and Electronic Structures, Phase Ranges, and Electrical and Magnetic Properties. *Eur. J. Inorg. Chem.* **2000**, 315.
- (10) Takeda, N.; Ishikawa, M. Superconducting and Magnetic Properties of Filled Skutterudite Compounds $\text{RERu}_4\text{Sb}_{12}$ (*RE* = La, Ce, Pr, Nd and Eu). *J. Phys. Soc. Jpn.* **2000**, *69*, 868.
- (11) Luo, H.; Krizan, J. W.; Muechler, I.; Haldolaarachchige, N.; Klimczuk, T.; Xie, W.; Fucillo, M. K.; Felser, C.; Cava, R. J. A Large Family of Filled Skutterudites Stabilized by Electron Count. *Nat. Commun.* **2015**, *6*, 6489.
- (12) Rietveld, H. M. A Profile Refinement Method for Nuclear and Magnetic Structures. *J. Appl. Crystallogr.* **1969**, *2*, 65.
- (13) Rodríguez-Carvajal, J. Recent Advances in Magnetic Structure Determination by Neutron Powder Diffraction. *Phys. B: Condens. Matter* **1993**, *192*, 55.
- (14) Waser, J. Least-squares Refinement with Subsidiary Conditions. *Acta Crystallogr.* **1963**, *16*, 1091.
- (15) Sheldrick, G. M. A short history of SHELX. *Acta Crystallogr., Sect. A* **2008**, *64*, 112.
- (16) Schwarz, K.; Blaha, P. Solid State Calculations using WIEN2k. *Comput. Mater. Sci.* **2003**, *28*, 259.
- (17) Kresse, G.; Furthmüller, J. Efficient Iterative Schemes for *ab-initio* Total-energy Calculations Using a Plane-wave Basis Set. *Phys. Rev. B* **1996**, *54*, 11169.
- (18) Monthoux, P.; Balatsky, A. V.; Pines, D. Weak-coupling Theory of High-temperature Superconductivity in the Antiferromagnetically Correlated Copper Oxides. *Phys. Rev. B* **1992**, *46*, 14803.
- (19) McMillan, W. L. Transition Temperature of Strong-Coupled Superconductors. *Phys. Rev.* **1968**, *167*, 331.
- (20) Bardeen, J.; Pines, D. Electron-Phonon Interaction in Metals. *Phys. Rev.* **1955**, *99*, 1140.
- (21) Marder, M. P. *Condensed Matter Physics*; John Wiley & Sons: 2010.